



# The impact of stochastic physics on the El Niño Southern Oscillation in the EC-Earth coupled model

Chunxue Yang<sup>1,5</sup> · Hannah M. Christensen<sup>2,3</sup> · Susanna Corti<sup>1</sup> · Jost von Hardenberg<sup>4</sup> · Paolo Davini<sup>4</sup>

Received: 7 March 2018 / Accepted: 1 February 2019 / Published online: 7 February 2019  
© The Author(s) 2019

## Abstract

The impact of stochastic physics on El Niño Southern Oscillation (ENSO) is investigated in the EC-Earth coupled climate model. By comparing an ensemble of three members of control historical simulations with three ensemble members that include stochastic physics in the atmosphere, we find that in EC-Earth the implementation of stochastic physics improves the excessively weak representation of ENSO. Specifically, the amplitude of both El Niño and, to a lesser extent, La Niña increases. Stochastic physics also ameliorates the temporal variability of ENSO at interannual time scales, demonstrated by the emergence of peaks in the power spectrum with periods of 5–7 years and 3–4 years. Based on the analogy with the behaviour of an idealized delayed oscillator model (DO) with stochastic noise, we find that when the atmosphere–ocean coupling is small (large) the amplitude of ENSO increases (decreases) following an amplification of the noise amplitude. The underestimated ENSO variability in the EC-Earth control runs and the associated amplification due to stochastic physics could be therefore consistent with an excessively weak atmosphere–ocean coupling. The activation of stochastic physics in the atmosphere increases westerly wind burst (WWB) occurrences (i.e. amplification of noise amplitude) that could trigger more and stronger El Niño events (i.e. increase of ENSO oscillation) in the coupled EC-Earth model. Further analysis of the mean state bias of EC-Earth suggests that a cold sea surface temperature (SST) and dry precipitation bias in the central tropical Pacific together with a warm SST and wet precipitation bias in the western tropical Pacific are responsible for the coupled feedback bias (weak coupling) in the tropical Pacific that is related to the weak ENSO simulation. The same analysis of the ENSO behaviour is carried out in a future scenario experiment (RCP8.5 forcing), highlighting that in a coupled model with an extreme warm SST, characterized by a strong coupling, the effect of stochastic physics on the ENSO representation is opposite. This corroborates the hypothesis that the mean state bias of the tropical Pacific region is the main reason for the ENSO representation deficiency in EC-Earth.

## 1 Introduction

The El Niño Southern Oscillation (ENSO) is the most prominent phenomenon in the tropical Pacific Ocean at interannual time scales (Rasmusson and Carpenter 1982). The effects of ENSO are not only significant at a local scale, as for example in South America (Sarachik and Cane 2010), but they impact also the global scale through ENSO teleconnections (Philander 1990), including effects on the intensity of precipitation in the Indian monsoon (Ropelewski and Halpert 1996) and in North Atlantic hurricanes (Bove et al. 1998). Due to the crucial role of ENSO in the global climate system, a large body of literature has been published in the last few decades to study different aspects of ENSO.

To this day the fundamental dynamics of ENSO still draws the attention of scientists: a number of theories have been proposed, the most influential of which are the

---

✉ Chunxue Yang  
chunxue.yang@artov.isac.cnr.it

<sup>1</sup> Istituto di Scienze dell'Atmosfera e del Clima, Consiglio Nazionale delle Ricerche (ISAC-CNR), Bologna, Italy

<sup>2</sup> Atmospheric, Oceanic and Planetary Physics, University of Oxford, Oxford, UK

<sup>3</sup> National Center for Atmospheric Research, Boulder, CO, USA

<sup>4</sup> Istituto di Scienze dell'Atmosfera e del Clima, Consiglio Nazionale delle Ricerche (ISAC-CNR), Torino, Italy

<sup>5</sup> Istituto di Scienze Marine, Consiglio Nazionale delle Ricerche (ISMAR-CNR), Via del Fosso del Cavaliere, 100, 00133 Rome, Italy

delayed oscillator model (Suarez and Schopf 1988; Battisti and Hirst 1989) and the recharge-discharge oscillator framework (Jin 1997a, b).

The delayed oscillator model has been introduced by Suarez and Schopf (1988). They demonstrated that a spontaneous oscillation could be provided by an adjustment of the ocean subsurface (i.e. the thermocline): Rossby waves propagate from the area of wind stress anomalies to the western boundary of the basin, before they damp the perturbation on their return to the eastern boundary as they are reflected as Kelvin waves. The occurrence of the oscillation depends on the coupling strength between ocean and atmosphere: below a critical coupling strength, no spontaneous oscillations are observed. With a hybrid coupled model, in which an ocean Global Circulation Model (GCM) is coupled with a simple atmosphere model, Neelin (1990) found that a more realistic atmosphere–ocean system also undergoes a Hopf bifurcation from a stable ocean state to a sustained ENSO oscillation. The amplitude, period and eastward extension of the oscillation increase along with the increasing coupling strength, and the ENSO oscillation ultimately becomes unstable to a higher frequency coupled mode.

On the other hand, the recharge-discharge oscillator was independently proposed by Cane and Zebiak (1985) and Wyrki (1985). In this theory the equatorial heat content is discharged (recharged) during a warm (cold) ENSO phase due to mass exchange between equatorial and off-equatorial regions associated with central Pacific wind anomalies and eastern Pacific Sea Surface Temperature (SST) anomalies (see also Jin 1997a, b).

Another key aspect of ENSO theory concerns the role of stochastic forcing, which has been widely discussed in several studies. For instance, Zebiak (1989) argued that stochastic forcing such as Westerly Wind Bursts (WWBs) have only modest effects in the Cane–Zebiak model (Cane and Zebiak 1985). Penland and Sardeshmukh (1995) by using an empirical model suggested that ENSO variability is due to several decaying modes maintained by atmospheric stochastic forcing. Chang et al. (1996), Jin et al. (1996) and Blanke et al. (1997) all found that a stable ENSO system could be maintained by noise from different perspectives. Several other studies also support the theory that WWBs that occur in the western tropical Pacific may play an important role in ENSO dynamics (Fedorov 2002; Lengaigne et al. 2004; Gebbie et al. 2007), and can trigger El Niño events on some occasions. A recent study by Fedorov et al. (2015) suggests that stochastic processes may be responsible for the diversity of El Niño. Evidences show that the amplitude of ENSO decadal variability is a result of stochastic forcing (Flugel et al. 2004; Yeh and Kirtman 2006), while Eisenman et al. (2005) argue that WWBs should not be treated as pure stochastic forcing and might be influenced by the ENSO. More

in general, the importance of stochastic forcing is recognized by the ENSO community.

Numerical representation of ENSO is also essential but still problematic. Indeed, state-of-the-art coupled global climate models show systematic errors in simulating ENSO (Guilyardi et al. 2009). The representation of ENSO is sensitive to details of the convection parameterization. For example, Neale et al. (2008) found that changing the deep convection parameterization resulted in an improvement of the ENSO representation in the Community Climate System Model version 3 (CCSM3). Despite model improvements in the last few decades, the representation of ENSO is still biased in several coupled climate models, including errors in the amplitude, in the spatial structure and the temporal variability as well as in representation of the asymmetry of El Niño and La Niña (Flato et al. 2013; Yang and Giese 2013).

One recent important breakthrough for numerical weather prediction models was the development of stochastic parameterization schemes at the European Centre for Medium-Range Weather Forecasts (ECMWF) (Palmer et al. 2009; Buizza et al. 1999). These schemes represent the variability of unresolved atmospheric processes. It has been demonstrated that stochastic physics improves the spread and mean state of seasonal and medium range forecasts, and so it has been included in forecast models worldwide (Palmer et al. 2009; Yonehara and Ujiie 2011; Bouttier et al. 2012; Weisheimer et al. 2014; Berner et al. 2012; Sanchez et al. 2016; Jankov 2017). Previous studies also show that including stochastic parameterizations of unresolved processes in atmospheric models can reduce model biases by improving both mean climate and climate variability (Sardeshmukh et al. 2001, 2003; Williams 2012; Berner et al. 2008, 2017; Lin and Neelin 2000, 2003).

In coupled climate models, the impact of stochastic physics, especially with the schemes originally developed for initialised forecasts, has not yet been widely explored. In Christensen et al. (2017), the Community Climate System Model version 4 (CCSM4) was used to investigate the impact of stochastic parameterization schemes on the representation of ENSO in coupled climate simulations. The results show that the use of the multiplicative stochastically perturbed parameterization tendencies (SPPT) scheme in the Community Atmosphere Model (CAM, the atmospheric component of CCSM) improves significantly the ENSO power spectrum by reducing the excessive power at periods of 3–4 years and increasing the power with periods less than 3 years. The overestimated ENSO magnitude, especially the amplitude of La Niña events, found in the control simulation of CCSM is also reduced by implementing the SPPT scheme. It is thus hypothesized that this change is due to the model's improved zonal wind variability, achieved by perturbing the convective heating tendencies, resulting in an improved ENSO variability.

This study is following the footsteps of Christensen et al. (2017). We will analyze the impact of stochastic physics on the ENSO representation in the EC-Earth coupled climate model and discuss the mechanisms behind it. The following sections describe the datasets used in the study (Sect. 2), and the impact of stochastic physics on ENSO in the EC-Earth model (Sect. 3). Finally, Sect. 4 provides a discussion and the conclusions.

## 2 Data and methods

The data used for this study come from simulations produced within the Climate Stochastic Physics HIgh resolution eXperiments (SPHINX) project. The details of the experiments are given in Davini et al. (2017). In this study, we use three coupled control experiments (CTRL) along with three coupled experiments (STO\_PHY) with stochastic physics, covering the period from 1850 to 2100. The EC-Earth coupled global climate model (version 3.1) is based on the Integrated Forecast System (IFS, cycle 36r4) (ECMWF, 2009) atmospheric model and on the Nucleus for European Modelling of the Ocean (NEMO 3.3.1; Madec, 2008) ocean model coupled, with the LIM3 sea ice model (Vancoppenolle et al. 2012). The coupler between atmospheric and ocean components is OASIS3 (Valcke 2013). The resolution of IFS is defined by a linear triangular truncation retaining 255 harmonics (T255) with 91 vertical levels (L91) which are represented in a hybrid coordinate system with the top level at 0.01 hPa. The output is interpolated onto a regular Gaussian grid with  $512 \times 256$  grid points (a resolution of about 80 km at the Equator). The configuration of NEMO is based on ORCA1L46, with an average horizontal resolution of  $1^\circ$  (zonal)  $\times$   $1^\circ$  (meridional) and 46 vertical depth levels.

The forcing for the experiments is from the fifth Coupled Model Intercomparison Project (CMIP5, Taylor et al. 2012). From 1850 to 2005 the forcing, including greenhouse gases, ozone concentrations and volcanic aerosols, is based on the CMIP5 historical forcing set up, and from 2006 to 2100 the forcing is based on the CMIP5 RCP8.5 scenario set up. Two sets of 320 years preindustrial spin up for both the CTRL and the STO\_PHY runs were conducted, in order to reach an equilibrated ocean state. Year 300, 310 and 320 of the spin up experiments are used as initial conditions for each ensemble member starting from 1840 for both the control and the perturbed runs. From 1840 to 1850 a constant forcing for year 1850 is applied, in order to allow for a further 10-years spin up in order to let the atmosphere and land surface to adjust to the new oceanic state (Davini et al. 2017). In this study, we choose the period from 1870 to 2009 as historical runs and the period from 2010 to 2100 as future scenario runs.

In the STO\_PHY runs both the stochastically perturbed parameterization tendencies (SPPT) scheme with multiplicative noise and the Stochastic Kinetic Energy Backscatter (SKEB) scheme (Palmer et al. 2009) are implemented. The schemes aim to represent the model error (uncertainty) associated with the parameterization schemes of sub-grid physical processes. The SPPT scheme focuses on the uncertainty arising from the existing sub-grid parameterization schemes (including radiation, clouds, convection, turbulence and boundary layer processes, and gravity wave drag) using a multiplicative noise approach. More specifically, the SPPT scheme is applied to parameterized tendencies of the four prognostic variables temperature (T), horizontal and meridional wind (u, v) and specific humidity (q) are multiplied by the same random number, r

$$X_p = (1 + r\mu)X_c, \quad (1)$$

in which  $X_p$  are the parameterized tendencies of perturbed fields and  $X_c$  are the unperturbed (deterministic) parameterized tendencies, both of which vary as a function of time, spatial location and model level.  $\mu \in [0, 1]$  is a factor, constant in time and horizontal position, that smoothly reduces the perturbation amplitude to zero close to the surface and in the stratosphere. The perturbation r follows a Gaussian distribution, is constant with height but is correlated in space, follows a first order auto-regressive process in time, and is generated through a spectral pattern generator as described in Berner et al. (2008).

The SKEB scheme is designed to represent upscale transfer of energy that is observed in the real atmosphere, but absent in forecast models (Berner et al. 2008). It estimates the kinetic energy lost in the model due to dissipation at the smallest scales, and scatters this energy upscale through perturbing the streamfunction at the largest scales. The streamfunction perturbations are modulated using the same stochastic spectral pattern as for SPPT, except that the perturbation varies in height as well as space. For more details, see Berner et al. (2008). While the stochastic physics runs presented here include both the SPPT and SKEB scheme, previous work indicates that the impact of the SKEB scheme is modest compared to SPPT in the IFS (Weisheimer et al. 2014). We therefore focus on the SPPT scheme in our discussion.

Since stochastic physics is only implemented in the atmospheric component of the EC-Earth, we make use of another set of the Climate SPHINX runs which includes a series of atmosphere standalone experiments (carried out with the atmospheric component of EC-Earth, see Davini et al. 2017 for more details), aiming at investigating the impact of stochastic physics when the atmospheric model is forced by a fixed SSTs (i.e. when there is no mutual interaction between ocean and atmosphere). The boundary conditions of the atmosphere-only runs come from the

Hadley Centre Sea Ice and Sea Surface Temperature data set (HadISST 2.1.1, Titchner and Rayner 2014). We consider ten ensemble members for control and ten members with stochastic physics with the same horizontal and vertical resolution as the coupled runs; each experiment covers the period 1979 to 2008. The initial condition of atmosphere-only experiment comes from ERA-Interim for 01/01/1979 from each a first ensemble member is run. Then, initial conditions for the other ensemble members are extracted from the midnight values (00:00) of the first 10 days of the first integration (Davini et al. 2017).

Finally, the observations and reanalyses for comparison in this study include the HadISST1 (Rayner et al. 2003) and Global Precipitation Climatology Project (GPCP) (Alder et al. 2003) datasets.

### 3 Results

#### 3.1 The response of ENSO to stochastic physics

In order to evaluate the impact of stochastic physics on ENSO, first we calculate the composite of El Niño and La Niña events for the period of 1870–2009. The definition of ENSO is based on the Niño 3.4 index, which is the SST anomaly (December, January and February months) averaged in the box 170°W–120°W, 5°S–5°N. An El Niño event is defined when the Niño 3.4 index is larger than 0.5 °C and a La Niña event when the index is lower than –0.5 °C. In Fig. 1 we show results for HadISST1 and for the ensemble mean of the three ensemble members for both control (CTRL) and stochastic physics (STO\_PHY) runs, in the historical experiments (1870–2009), as well as their differences. Compared with HadISST1 (Fig. 1g, h), both the El Niño and La Niña composites in the control run are weaker. In particular, even if in the central eastern tropical Pacific Ocean the maximum of the amplitude of El Niño and La Niña is comparable with that in HadISST1, in the central western tropical Pacific Ocean the amplitude is much weaker.

In the STO\_PHY runs the amplitude of the El Niño composites increases in the tropical Pacific (Fig. 1c, e, i), even though it is still weaker than in HadISST1. Specifically, the maximum of El Niño expands from the central eastern towards to the central western tropical Pacific Ocean. For the La Niña composite (Fig. 1d, f, j), the increase of amplitude slightly weaker than for El Niño. The main improvement is the location of maximum amplitude which extends further south and north, and further towards the central western tropical Pacific.

More in general, with stochastic physics, the typical SST ‘horseshoe’ pattern observed during El Niño and La Niña is closer to that found in HadISST and the warm anomaly in

the western tropical Pacific is reduced as well (Fig. 1g, i, j). These variations are statistically different from zero above the 95% level (grey areas in Fig. 1i, j) over the western tropical Pacific Ocean, where the biases are large and, in general, over most of the tropical Pacific with the exception of the southern central region.

The asymmetric improvement of El Niño and La Niña with stochastic physics in climate models (see also Christensen et al. 2017) implies an improvement in the representation of asymmetry of El Niño and La Niña, a feature that is generally not well simulated by climate coupled models (Yang and Giese 2013; Zhang and Sun 2014). The composite Hovmöller diagrams of El Niño and La Niña (Fig. 2) calculated for the historical period (1870–2009) shows that the amplitude of El Niño increases with stochastic physics, such that the amplitude of the modelled El Niño becomes closer to that observed. In contrast, the maximum amplitude of La Niña does not change significantly, but rather shifts westward towards the central Pacific. This agrees with Fig. 1 and confirms that the improvement of El Niño and La Niña due to the stochastic physics is asymmetric. The ENSO variability, calculated as the timeseries of the standard deviation of monthly means of the Niño 3.4 index, is shown in Fig. 3. Here EC-Earth with (STO\_PHY, red line) and without stochastic physics (CTRL, blue line) is compared against HadISST1 data (black line). The variability of ENSO in CTRL is weaker than HadISST1, with a minimum during July. With stochastic physics the amplitude of variability of ENSO increases for all the months, though the minimum of variability is still during July instead of late spring as in HadISST1.

The temporal variability of ENSO is further inspected analyzing the ENSO power spectrum (Fig. 4). The ensemble mean power spectrum from the three control experiments is weaker and flatter (black solid line) than HadISST1 (grey line), especially for the pronounced peak within 2–7 year period. Previous studies show that in general the CMIP5 coupled models have a narrow and sharp power spectrum bias (Flato et al. 2013; Christensen et al. 2017). On the contrary, in EC-Earth the power spectrum of ENSO is flat and weak.

The power spectrum is considerably different for the STO\_PHY runs: here the spectral amplitude of ENSO increases, with the two peaks at 3–4 and 5–7 years periods (seen in HadISST1) emerging from the background.

Based on the discussion above, it appears clear that stochastic physics has important beneficial impacts in the simulation of ENSO in terms of amplitude and spectrum in the EC-Earth climate model. Two questions follow immediately: what is the mechanism leading to such an impact of stochastic physics on ENSO in EC-Earth? And why is this completely opposite to the one observed in CCSM (as discussed in the Sect. 1 and shown in Christensen et al.



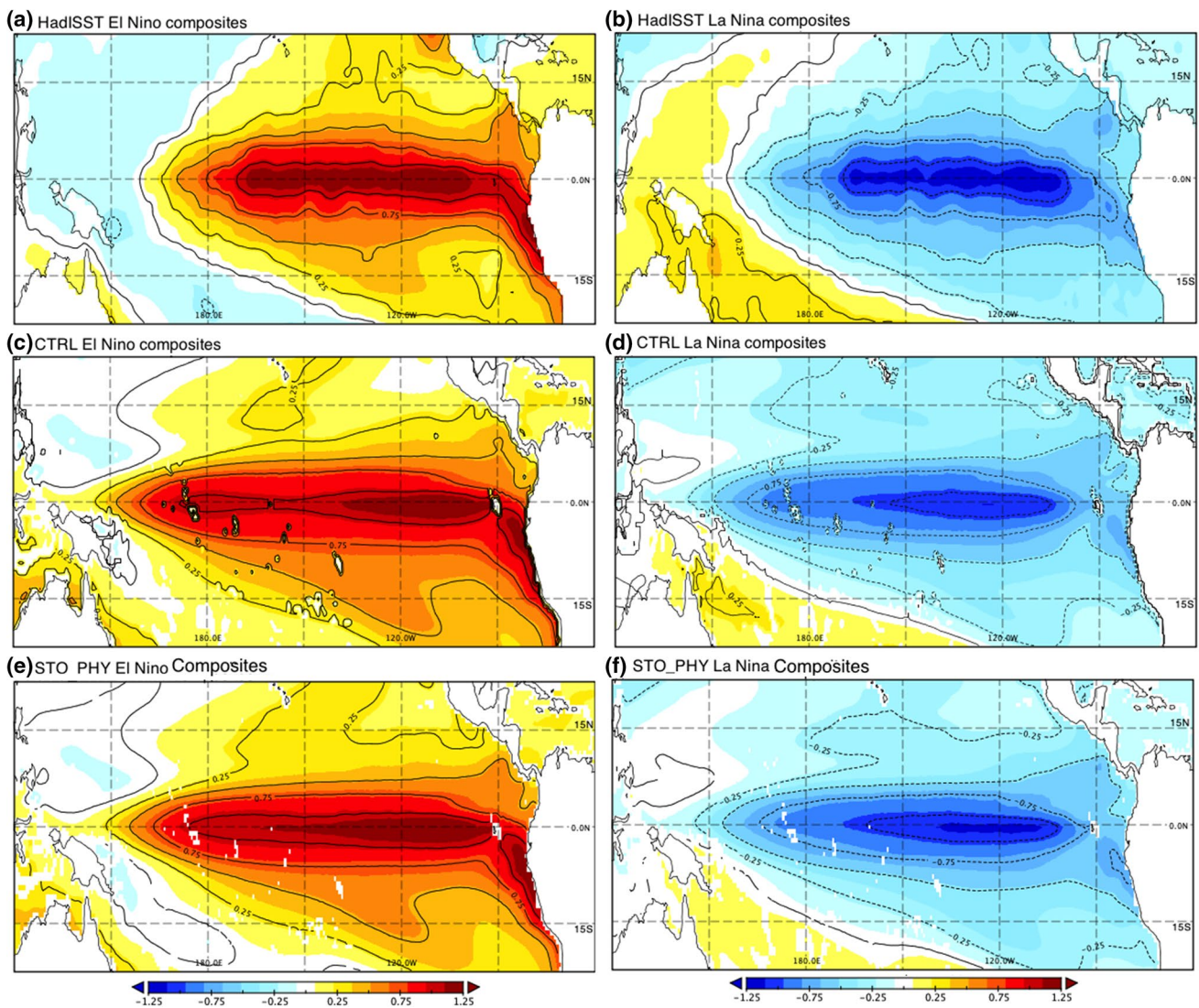


**Fig. 1** Sea surface temperature (SST) composites (1870–2009) of El Niño events in **a** HadISST1, **c** CTRL and **e** STO\_PHY runs and composites of La Niña events in **b** HadISST1, **d** CTRL and **f** STO\_PHY runs. Difference between CTRL and HadISST for El Niño (**g**) and La

Niña (**h**) composites. Difference between STO\_PHY and CTRL for El Niño (**i**) and La Niña composites (**j**). Grey shaded areas in **i** and **j** show where differences are significantly different from zero above the 95% level according to the Student *t* test

2017), even considering that in both models the ENSO representation is improved?

Indeed, in the CCSM model the power spectrum of ENSO (see Fig. 3 in Christensen et al. 2017) is narrow and sharp with a dominant period of 3–4 years. With stochastic physics, the power spectrum is improved by reducing the dominant power in 3–4 years oscillation and increasing power in high frequency oscillation. Furthermore, in the CCSM the application of stochastic physics reduces the strong La Niña bias present in the CTRL experiments, but has little impact on El Niño amplitude contrast in EC-Earth the stochastic physics increases the amplitude of El Niño but has little impact on La Niña.

The following sections will investigate the source of these contrasting effects of stochastic physics when implemented in different coupled climate models.

### 3.2 Delayed oscillator model and stochastic perturbation

#### 3.2.1 Delayed oscillator

According to the ENSO theory proposed in the literature, as outlined in the introduction, there are two main factors that affect ENSO: the ocean–atmosphere coupling strength, and the stochastic forcing present in the system.

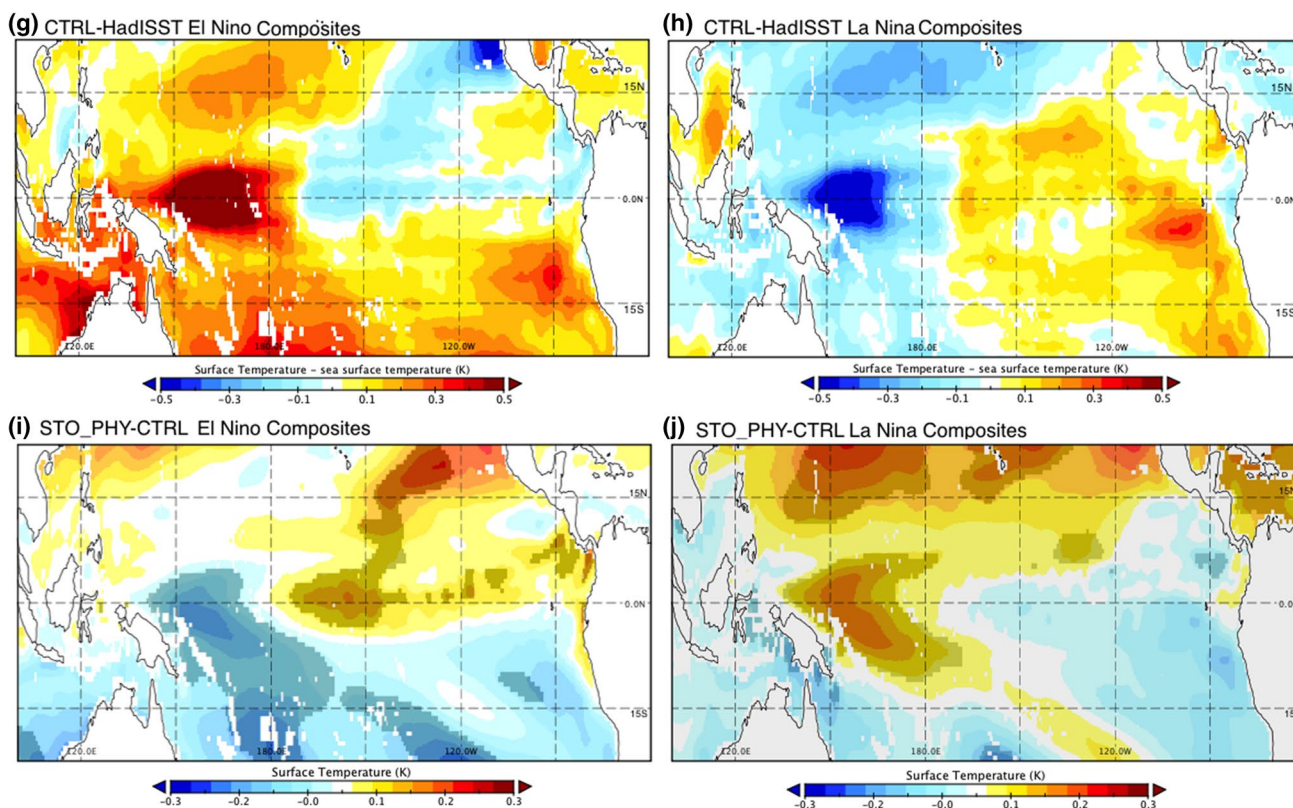


Fig. 1 (continued)

Christensen et al. (2017) argued that CCSM shows a narrow and sharp ENSO spectrum because of the relatively strong ocean–atmosphere coupling in CCSM. This strong ocean–atmosphere coupling results in a regular, self-sustaining ENSO. The input of multiplicative noise introduced by the stochastic parameterization reduces the coupling strength in CCSM, leading to an improvement of ENSO. On the other hand, in the EC-Earth control simulations the ENSO power spectrum and amplitude are weaker than in the real world. This might be due to excessively weak ocean–atmosphere coupling which leads to a weaker ENSO oscillation. By (linear) analogy with the impact of stochastic physics on CCSM, a further weakening of ENSO should be expected when stochastic perturbations are included in EC-Earth. However, as reported in the previous section, the impact of stochastic physics on ENSO in EC-Earth is the opposite to CCSM: in EC-Earth the inclusion of multiplicative noise does amplify the ENSO oscillation (while it damps and disturbs the too regular self-sustaining ENSO in CCSM). In both models though, the changes induced by stochastic physics, even if opposite, translate in a net improvement of ENSO representation.

We attempt to explain these counterintuitive results making use of the analogy with the behaviour of a simple Delayed Oscillator (DO) model. The delayed oscillator (DO)

model is based on Stone et al. (1998), which is a simplified version of that presented by Munnich et al. (1991). The details of the DO model were introduced in Christensen et al. (2017). This is a one dimensional model describing the evolution of eastern Pacific thermocline depth anomaly with time ( $h(t)$ ), which represents the oscillation of ENSO amplitude calculated as the deviation from the seasonal thermocline depth value at the eastern boundary. The DO model is based on four parts, including (1) the effect of a Kelvin wave travelling to the eastern boundary, (2) a Rossby wave travelling to the western boundary and (3) reflected as Kelvin wave travelling to the eastern boundary as well as (4) the effect of the annual cycle. A stochastic perturbation is included using the following equation.

$$\kappa_s = [1 + cD\xi(t)]\kappa. \quad (2)$$

The  $\kappa$  parameter represents the coupling strength between ocean and atmosphere, that summarize all the ocean processes that affect the wind stress (Cane et al. 1990).  $\kappa_s$  determines the instantaneous strength of ocean–atmosphere coupling including the impact of multiplicative noise. This stochastic perturbation, which is represented as  $cD\xi(t)$  was designed to mimic the impact of the SPPT scheme on a climate model (Christensen et al. 2017).  $\xi$  is Gaussian distributed white noise, with mean ( $\xi$ ) = 0 and Var ( $\xi$ ) = 1



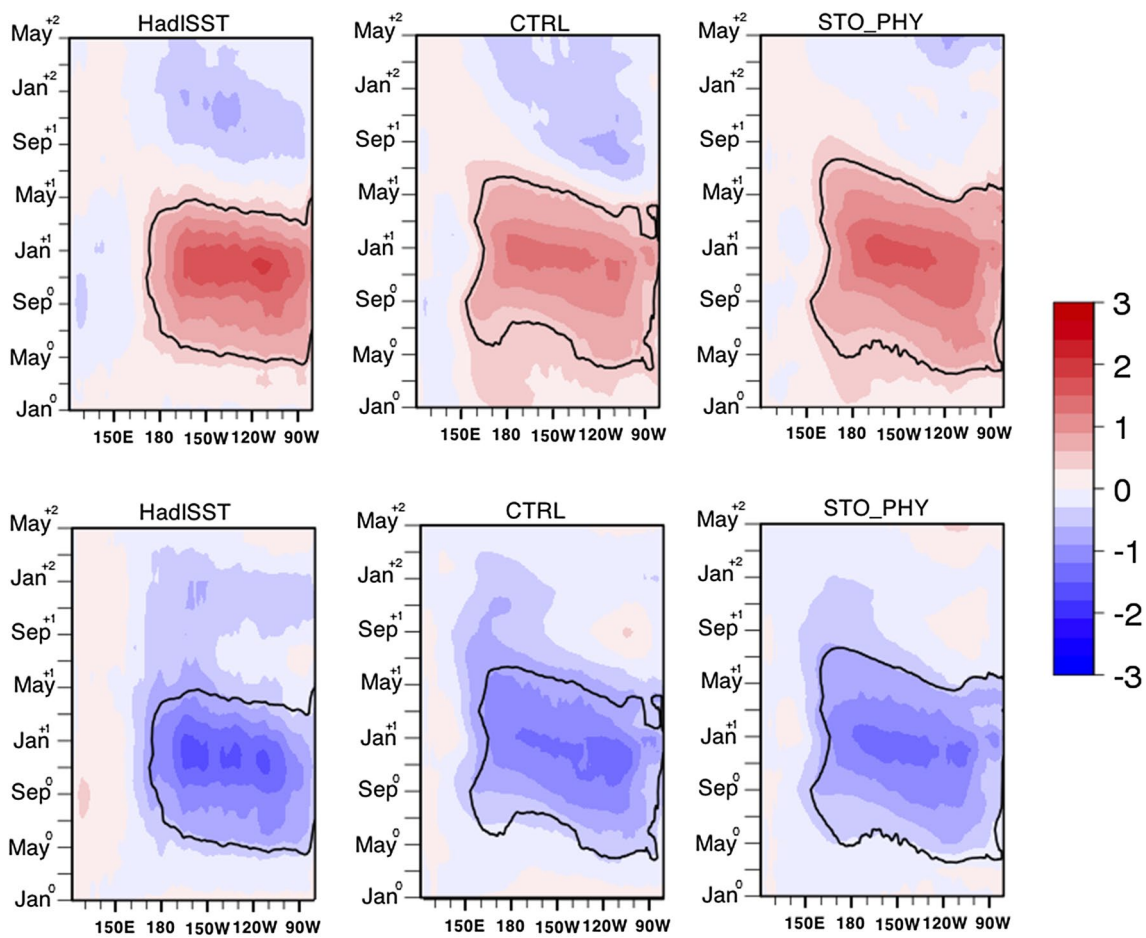


**Fig. 2** Hovmöller diagrams of El Niño composites (upper panel) and La Niña composites (lower panel) for HadISST, ensemble mean CTRL and ensemble mean STO\_PHY. SSTs are averaged between 5°S and 5°N

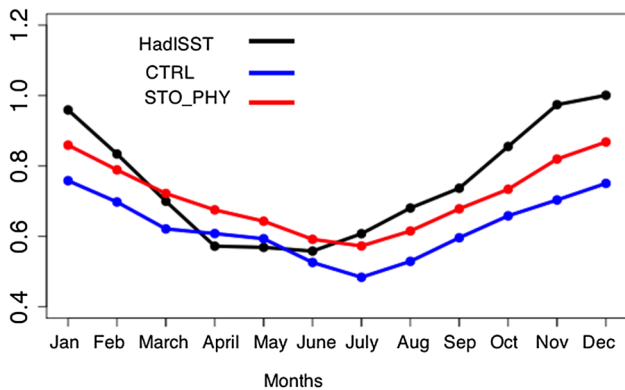


**Fig. 3** The monthly variability of ENSO based on Niño 3.4 index in HadISST (black), ensemble mean CTRL (blue) and ensemble mean STO\_PHY (red)

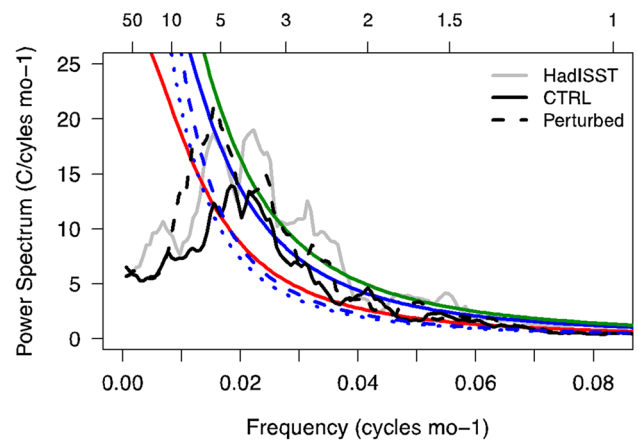


**Fig. 4** The power spectrum of the Niño 3.4 timeseries in ensemble mean CTRL (solid black), ensemble mean STO\_PHY (dashed black) and HadISST1 (grey). The best fit AR(1) spectrum (red) and its 95% (blue) and 99% (green) confidence bounds for HadISST. Dashed and dotted blue lines are the 95% confidence bounds for STO\_PHY and CTRL

and uncorrelated in time,  $\xi$  represents the amplitude of the multiplicative noise injected into the system relative to the seasonal cycle, and  $c$  is the amplitude of the seasonal cycle.

The purpose of using the DO model is to investigate the mechanisms of the impact of stochastic physics on ENSO with a simple model. Figure 5 shows the impact of the ocean–atmosphere coupling strength ( $x$ -axis as  $\kappa_s$ ) and the amplitude of the multiplicative noise term on the ENSO oscillation amplitude, as represented by the thermocline depth anomaly change ( $y$ -axis as  $h(t)$ ). The coloured lines in Fig. 5 indicate increasing values of the parameter  $D$ . The DO model undergoes a Hopf bifurcation as  $D$  increases with  $D=0$  (black line with circles) representing the unperturbed model. For weak ocean–atmosphere coupling (low  $\kappa_s$ ), the DO model only has an annual cycle without the signal of ENSO oscillation. With increasing  $\kappa_s$  above the critical value of 1.335, the ENSO oscillation emerges in the DO model.

The impact of additional multiplicative noise forcing is considered. Including even a small-amplitude multiplicative noise forcing can induce spontaneous ENSO-like oscillations below the bifurcation point, i.e. for  $\kappa_s < 1.335$ . An interesting feature emerging from Fig. 5 is that the change of the ENSO amplitude along with increasing stochastic forcing amplitude is not a linear function of  $\kappa_s$ . Close to the bifurcation point, the oscillation is chaotic. Away from the bifurcation point, with weak coupling strength (small  $\kappa_s$  values) the ENSO amplitude increases with increasing multiplicative noise forcing, while for strong coupling (large  $\kappa_s$  values above 1.34) the ENSO amplitude decreases with increasing amplitude of multiplicative noise forcing.

As discussed above, by applying stochastic physics, the ENSO oscillation amplitude increases in EC-Earth and decreases in CCSM. Thus, by analogy with the behaviour of the DO model, it might be possible that EC-Earth falls into the weak-coupling category (possibly close to the

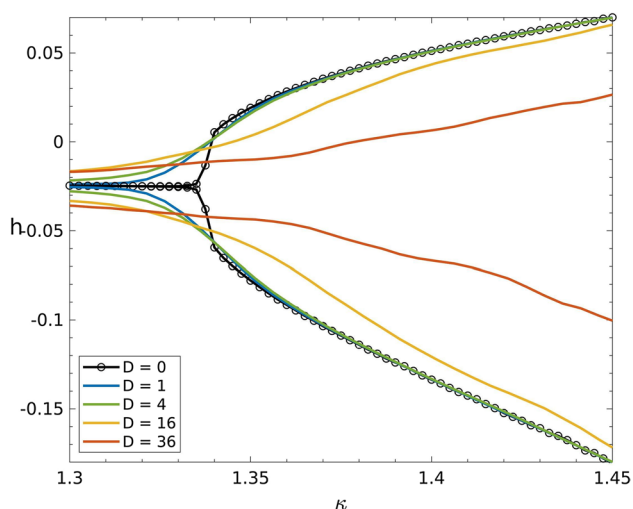


**Fig. 5** The change of thermocline depth,  $h(t)$ , in the DO model, shown as a function of  $\kappa_s$  for different amplitudes of noise. Parameter  $\kappa_s$  sets the strength of the ocean–atmosphere coupling,  $D$  sets the amplitude of the multiplicative noise with respect to the annual cycle

bifurcation point). In contrast, CCSM might belong to the strong-coupling category of coupled climate models.

Previous studies also proposed that errors in the coupled feedback processes could be the reason for the ENSO diversity in different climate coupled models (Philip et al. 2010; Lloyd et al. 2011). In the case of weak coupling, as supposed for EC-Earth, stochastic physics may excite the growth of non-normal modes in the system (Penland and Sardeshmukh 1995), thus resulting in an improvement of ENSO.

### 3.2.2 The impact of stochastic physics on WWBs

We now consider the physical mechanisms by which stochastic physics improves the representation of ENSO in EC-Earth. The most effective of the two stochastic physics schemes implemented, i.e. the SPPT scheme, perturbs the parametrized tendencies of temperature, specific humidity, and zonal and meridional wind. Therefore, the variability of wind could be affected by the perturbation of the tendency, which may affect the frequency and strength of westerly wind bursts (WWB). This is known to be an important factor affecting ENSO frequency and amplitude (Fedorov 2002; Lengaigne et al. 2004; Gebbie et al. 2007). In coupled models, due to the atmosphere and ocean coupled feedback, it is not possible to isolate the impact of stochastic physics on the wind. For example, even though several studies showed that wind variability in the West Pacific is larger before El Niño onset, (e.g. Wieners et al. 2016), there are discussions (e.g. Eisenmann 2005) about whether the wind variability causes El Niño or vice versa. Therefore, following Christensen et al. (2017), we use atmosphere-only simulations to explore the direct impact of stochastic physics on WWB statistics. 5-day running mean and low frequency variability filter (a Butterworth filter over 1 year) is applied on daily data from CTRL and STO\_PHY simulations to highlight persistent wind anomalies. Wind speed larger than  $7 \text{ m s}^{-1}$  is required to define a WWB following Vecchi and Harrison (2000).

Figure 6a displays the probability density function of U850s in CTRL run (blue line), STO\_PHY (red line) and ERA-Interim Reanalysis (black). It is evident that with stochastic physics the frequency and strength of WWBs increases, even though both CTRL and STO\_PHY have more WWBs than ERA-Interim. In order to see the evolution of WWBs in time, the monthly averaged fractional area coverage of WWBs as a function of time is plotted in Fig. 6b. The fractional area coverage of WWBs is calculated only in the tropical region ( $5^\circ\text{N}$ – $5^\circ\text{S}$ ,  $130^\circ\text{E}$ – $260^\circ\text{E}$ ). The WWBs in the STO\_PHY simulation (red line) tend to be more prevalent than in the CTRL simulation. The variability of wind at 850 hPa (not shown) also increases with stochastic physics, especially in the western tropical Pacific, which is consistent with the increase of WWBs.



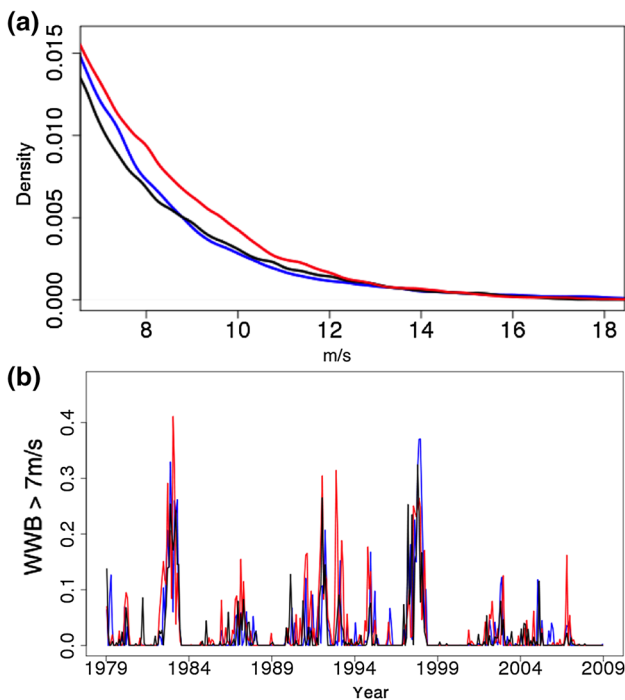


**Fig. 6** **a** The distribution of U850 (westerly wind) anomalies ( $\text{m s}^{-1}$ ) from the ERA-Interim dataset (black), ensemble mean CTRL (blue), and ensemble mean STO\_PHY (red). The data are first smoothed using a 5-day running mean and low frequency variability (over 1 year) is filtered out, and the PDFs are constructed using all spatial points between 5N and 5S and between 130E and 260E. **b** WWBs for the atmosphere-only integrations as a function of time for the ERA-Interim dataset (black), CTRL (blue), and STO\_PHY (red) model runs. The time series show the monthly average (130E–260E, 5S–5N) fraction of grid points that have a WWB (wind speed  $> 7 \text{ m s}^{-1}$ )

We note that the impact of stochastic physics on WWBs in the CCSM model is quite different to that in EC-Earth. In CCSM, stochastic physics improves the distribution of WWBs by reducing the (too high) frequency of wind anomalies above  $7 \text{ m s}^{-1}$  along with the stochastic component of their variability and decreasing the (too strong) correlation between SST and WWBs (see Figs. 11 and 12 in Christensen et al. 2017). The improved ENSO variability

in CCSM was attributed to these observed impacts on WWB, and it was suggested that a systematic reduction on the atmosphere–ocean coupling strength observed in the La Niña phase was the primary cause of the reduced ENSO amplitude in CCSM (Christensen et al. 2017). In EC-Earth the coupling between ocean and atmosphere, here represented by the coupling between SST and wind, could also be responsible for the increase of ENSO variability.

### 3.2.3 Assessing atmosphere–ocean coupling strength using a statistical model

The relationship between SST and wind in different simulations is further investigated by considering a simple statistical model for the dependency of zonal wind on SST anomaly. Following Levine et al. (2016), the wind speed in each simulation and in observations is represented as the sum of a deterministic ( $U_D$ ) and stochastic ( $U_S$ ) component so that:

$$U = U_D + U_S, \tag{3}$$

$$U_D = \mu_1 T + \mu_2 H(T)T + \mu_{AC} T \cos(\omega_{AC} t - t_{AC}), \tag{4}$$

$$U_S = \mu_S [1 + B H(T)T]. \tag{5}$$

The deterministic wind response has both a linear and threshold-nonlinear dependency on SST through the  $\mu_1$  and  $\mu_2$  parameters respectively, where  $H(T)$  is the Heaviside function, and a further deterministic dependency on the annual cycle ( $\mu_{ac}$ ), where  $t_{AC}$  is the number of months that the annual cycle is offset from the ENSO peak in ERA-interim. The stochastic component,  $U_S$ , is state dependent, with the parameter  $B$  determining the increased likelihood of stochastic WWBs with enhanced SSTs. The five parameters  $\mu_1, \mu_2, \mu_S, \mu_{AC}$  and  $B$  are fitted to timeseries of monthly SST and U850 anomalies averaged over  $3^\circ\text{S}$ – $3^\circ\text{N}$ ,  $160^\circ\text{E}$ – $200^\circ\text{E}$ , and their values shown in Fig. 7 for ERA-Interim (black), CTRL (blue) and STO\_PHY (red).

In the CTRL simulation, the parameters describing the strength of the deterministic feedback ( $\mu_1$  and  $\mu_2$ ) are lower than those fitted to ERA-interim (Fig. 7). The atmospheric

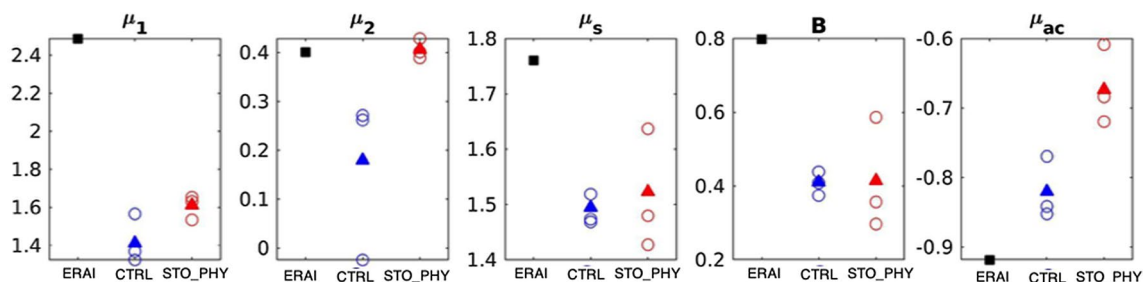


**Fig. 7** The relationship between WWBs and SST in terms of parameters following Levine et al. (2016), for ERA-Interim(ERAI, black), CTRL (blue) and STO\_PHY (red). The circles represent each ensemble member and the triangle represents the ensemble mean

wind response to a SST anomaly is weaker in EC-Earth than in observations, indicating a weaker atmosphere–ocean coupling. Note that this is in contrast to CCSM, which shows stronger deterministic feedback parameters than observations, indicating a stronger atmosphere–ocean coupling than in the observed ENSO, as previously discussed (Christensen et al. 2017; their Table 4).

Compared to the EC-Earth CTRL simulation, the parameters describing the strength of the deterministic feedback ( $\mu_1$  and  $\mu_2$ ) increase in STO\_PHY, indicating an enhancement in coupling strength between atmosphere and ocean. In particular, the  $\mu_2$  parameter shows a marked improvement in STO\_PHY compared to CTRL. This parameter describes the degree of deterministic, nonlinear amplification of the wind response above a particular SST threshold, and indicates an improved low-frequency wind response to the oceanic forcing. This strengthening of the coupling between SST and winds contributes to the increase in ENSO amplitude.

Interestingly, the parameters describing the stochastic component of the wind,  $\mu_s$  and B, show no significant difference between the CTRL and STO\_PHY simulation. On the timescale of the monthly mean fields used for this analysis, it appears that the stochastic parameterisations primarily affect the systematic response of the zonal wind to the ocean state, as opposed to fluctuations in the monthly mean wind. We note that the STO\_PHY run shows a poorer representation of ENSO-annual cycle combination tones [i.e. the enhanced spectral energy generated by the nonlinear modulation of ENSO by the seasonal cycle or vice versa (Timmermann et al. 2018)], with a weaker dependency of ENSO amplitude on these tones in the STO\_PHY simulation than in either CTRL or ERA-Interim. While this reduction in the phase-locking of ENSO will likely contribute to enhanced variability, compensating for the too low  $\mu_s$  and B parameters, this weakened dependency is undesirable. However, understanding the interaction of stochastic physics with the annual cycle, and thereby the reason for this impact, is beyond the scope of this study.

These results indicate an improved low-frequency wind response to the oceanic forcing, on top of which the high-frequency stochastic WWB forcing will act. The combination of strengthening of the coupling between SST and winds and the increase of WWBs (shown in Fig. 6) likely contributes to the increases of ENSO variability and amplitude.

### 3.3 The mean state of the tropical Pacific Ocean

The other question raised in this study is why the atmosphere and ocean in EC-Earth are weakly coupled, with an associated weak ENSO, but CCSM shows a strong atmosphere–ocean coupling and a correspondingly strong ENSO. Several studies have demonstrated that the mean state biases have a considerable impact on the atmosphere–ocean

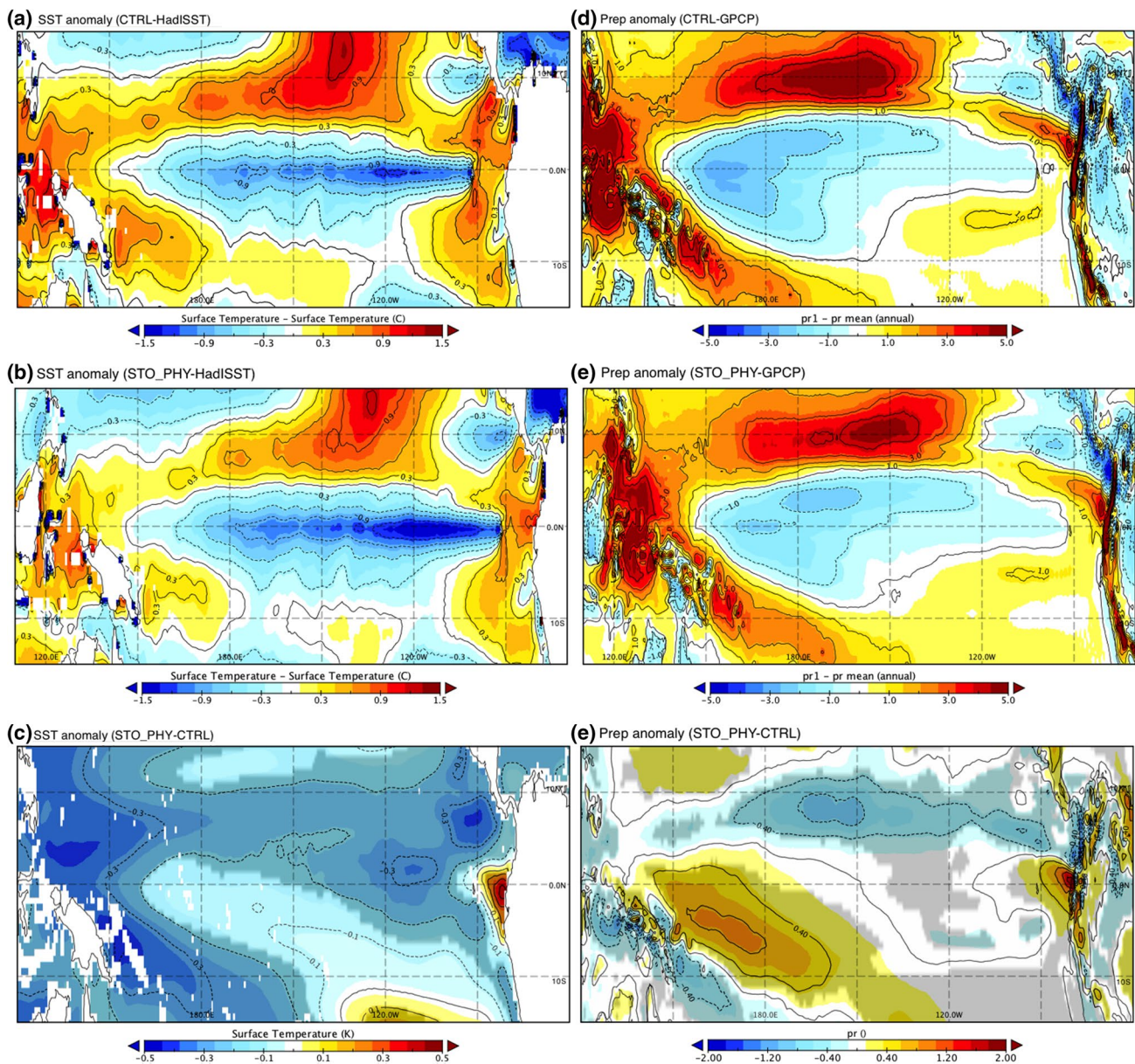
coupling strength (An et al. 2010; Watanabe and Wittenberg 2012; Watanabe et al. 2012) as well as on the ENSO variability (Ham and Kug 2014; Sriviver et al. 2014). Therefore, in EC-Earth, the mean state bias in the tropical Pacific could be a possible reason for the weak atmosphere–ocean coupling and the weak ENSO variability.

Figure 8 displays the SST (Fig. 8a) and precipitation (Fig. 8c) biases for EC-Earth. The SST bias is calculated as the difference between one ensemble member (with the other two ensemble members having similar biases) of the CTRL historical experiment and HadISST1, while the precipitation bias is the difference between one ensemble member of the CTRL historical experiment and GPCP. A band characterized by a cold SST bias in the Equatorial Pacific as well as a warm bias in the western warm pool region and along the west coast of Central and South America are evident. Pacific SST displays a warm SST anomaly to the north and to the south of the equatorial belt.

Concerning precipitation, there is a negative bias in the equatorial tropical Pacific opposite to a positive bias in the western tropical Pacific warm pool region and in the areas to the north and to the south of the tropical Pacific. The pattern of precipitation bias matches with the SST bias due to the atmosphere and ocean feedback. Indeed, cold SST biases are associated with negative precipitation anomalies and vice versa.

With stochastic physics, the mean state of EC-Earth is improved, principally in the warm pool and along the coastal regions of the South America in the eastern tropical Pacific where the SST warm biases are reduced. In the eastern tropical Pacific Ocean, the cool biases have slightly increased, but not as much as to offset the reduction of the warming biases in the western Pacific. Therefore, the inclusion of stochastic physics results in an eastern-western SST gradient decrease in the tropical Pacific. The improvement of the mean state of precipitation is even more prominent compared with the SST. The wet bias in the western tropical Pacific warm pool area and the northern and southern tropical Pacific are much reduced and the dry bias in the central western tropical Pacific is also improved. Overall the bias of the mean state of the tropical Pacific is reduced almost everywhere (with the exception of the East Pacific), when stochastic physics is included.

The bias shown in EC-Earth model is consistent with the discussion of the bias of coupled models in previous studies (Luo et al. 2005; An et al. 2010; Xiang et al. 2012). Namely, this bias in the tropical Pacific influences the simulation of ENSO by affecting the atmosphere and ocean coupling strength. The warmer western tropical Pacific warm pool may also be responsible to the symmetric El Niño and La Niña in EC-Earth (Sun et al. 2013). On the other hand, for the case of CCSM discussed in Christensen et al. (2017), the CTRL simulation is too cool and too



**Fig. 8** **a** The SST bias (CTRL-HadISST1) in EC-Earth, **b** the SST difference between STO\_PHY and HadISST, **c** the SST difference between STO\_PHY and CTRL. Unit is °C. **d** The precipitation bias (CTRL-GPCP), **e** the precipitation difference between STO\_PHY and

GPCP, **f** the precipitation difference between STO\_PHY and CTRL and shaded areas are over 95% significant level with student t-test. Unit is mm/day

dry in the eastern tropical Pacific, and this is ameliorated by the inclusion of stochastic physics (H. Christensen, pers. comm.). These biases are opposite in sign to those in EC-Earth, impacting the atmosphere–ocean coupling strength in CCSM in a consistent manner. The diversity of ENSO simulation in different coupled climate models due to the biases of the coupled feedbacks simulation in the coupled climate models has also been pointed out by previous studies (Collins et al. 2010; Philip et al. 2010; Lloyd et al. 2011).

In order to strengthen the argument that the mean state is one of the possible reasons for the deficiency of ENSO simulation in climate coupled models, we performed the same analysis considering the impacts of stochastic physics on ENSO with the Climate SPHINX future scenario coupled runs. The future scenario runs (CTRL\_RCP8.5) are forced following the RCP8.5 scenario thus simulating a global warming world. Therefore, these EC-Earth simulations can be treated as if they were performed using a coupled model with much warmer SST anomalies



compared to historical experiments as in the CCSM. In CTRL\_RCP8.5 the amplitude of both El Niño (Fig. 9c) and La Niña (Fig. 9d) is stronger than the CTRL historical experiments. Even if there is still a large uncertainty on the impacts of global warming on ENSO (e.g. Stevenson 2012), in the EC-Earth under a global warming scenario more extreme ENSO events are expected (Fig. 9). With stochastic physics, the amplitude of El Niño decreases significantly but the amplitude of La Niña is less affected, as seen in historical experiments. The change of the temporal variability of ENSO is shown in Fig. 10 for CTRL\_RCP8.5, STO\_PHY\_RCP8.5 and HadISST1. Overall the impact of stochastic physics on ENSO behaviour in the EC-Earth RCP8.5 scenario is very different compared to that seen in historical experiments. In the EC-Earth RCP8.5 scenario, very warm SST anomalies are associated with large El Niño events. This results in a very strong and sharp spectrum, which, far from becoming sharper with the inclusion of stochastic physics (as in the historical integrations), shows a slightly less prominent power spectrum at 3–4.5 years period. Furthermore, the standard deviation of Niño 3.4 in winter is slightly reduced in STO\_PHY (not shown). In these “climate change” simulations, the impact of stochastic physics on ENSO is more in agreement with that found in the CCSM model, where warm SST biases (warm SST anomalies in case of RCP8.5 scenario) were associated with strong El Niño events and a sharp narrow ENSO power spectrum. In CCSM stochastic physics led to a reduced amplitude of El Niño events and to a wider and flatter power spectrum (Christensen et al. 2017). However, in EC-Earth RCP8.5, the impact of stochastic physics on the power spectrum and standard deviation of Niño 3.4 is subtler than in CCSM such that longer simulations or more ensemble members would be needed to test the significance of such changes. Nevertheless, the effect of stochastic physics on ENSO in the warm EC-Earth RCP8.5 simulations is more consistent, though weaker, with that observed in CCSM than with that shown by EC-Earth historical simulations.

In general, our findings for CCSM and EC-Earth agree with the results of the delayed oscillator, namely that by applying stochastic noise in the weakly coupled model (e.g. EC-Earth) ENSO is strengthened and in the strongly coupled model (e.g. CCSM) ENSO is weakened. The ENSO amplitude change in both cases may be due to the stochastic forcing itself, however the above-described change in the mean state could also play a relevant role. This latter possibility suggests that differences in the mean states of climate models might partially affect the way a system responds to stochastic noise (and more generally to a given external forcing).

## 4 Discussions and conclusions

This study explores the impact of stochastic physics on ENSO in the EC-Earth coupled global climate model. Three ensemble members of a control (CTRL) historical experiment and three members with stochastic physics (STO\_PHY) in the atmosphere are analysed. The results show that with the inclusion of stochastic physics, both the amplitude and the temporal variability of ENSO are improved. The amplitude of both El Niño and La Niña increases (Figs. 1, 2), with more evident improvements for El Niño events when compared to HadISST1. The asymmetric response of El Niño and La Niña is possibly related to the reduction of warm biases in the western tropical Pacific.

Most importantly, the power spectrum of ENSO (Fig. 4), that in CTRL is weak and flat, shows an increase of the amplitude for interannual timescales when stochastic physics is included. The improvement of the ENSO power spectrum with the inclusion of stochastic physics in the atmospheric component is consistent with a previous study by Christensen et al. (2017) with the CCSM model. However, in that case the inclusion of stochastic physics in the atmospheric components of CCSM led to a reduction of the excessive power at 3–4 years. Overall, with stochastic physics, the simulation of ENSO in terms of the amplitude and frequency is improved in EC-EARTH. To explain these counterintuitive results a simple Delayed Oscillator (DO) model is used. When multiplicative noise (designed to mimic the SPPT scheme) is applied to the DO, the effect on the DO ENSO-like oscillations depends dramatically on the (portion of) parameter space which the model is visiting. In the DO model the parameter,  $\kappa$ , represents the degree of coupling between atmosphere and ocean. We find that stochastic perturbations increase the DO ENSO amplitude when the atmosphere–ocean coupling is weak, while they decrease the ENSO amplitude when the atmosphere–ocean coupling is strong. The potential for opposite impacts of stochastic physics on ENSO in climate models is consistent with the DO model, depending on whether the climate model exhibits strong or weak atmosphere–ocean coupling. The weak ENSO power spectrum in EC-Earth suggests that this model fits in the weak coupling “category”. To test this hypothesis, we consider a statistical model of the zonal wind response to a SST anomaly, fitted to both observations and model data. The feedback parameters fitted to EC-Earth data indicate a substantially weaker response of atmospheric winds to SST anomalies, supporting the hypothesis that EC-Earth has too-weak ocean–atmosphere coupling. Consistent with the DO model, stochastic physics leads to an enhancement of ENSO in EC-Earth.

The analysis of westerly wind bursts (WWBs) in atmosphere-only runs shows that there are more frequent and

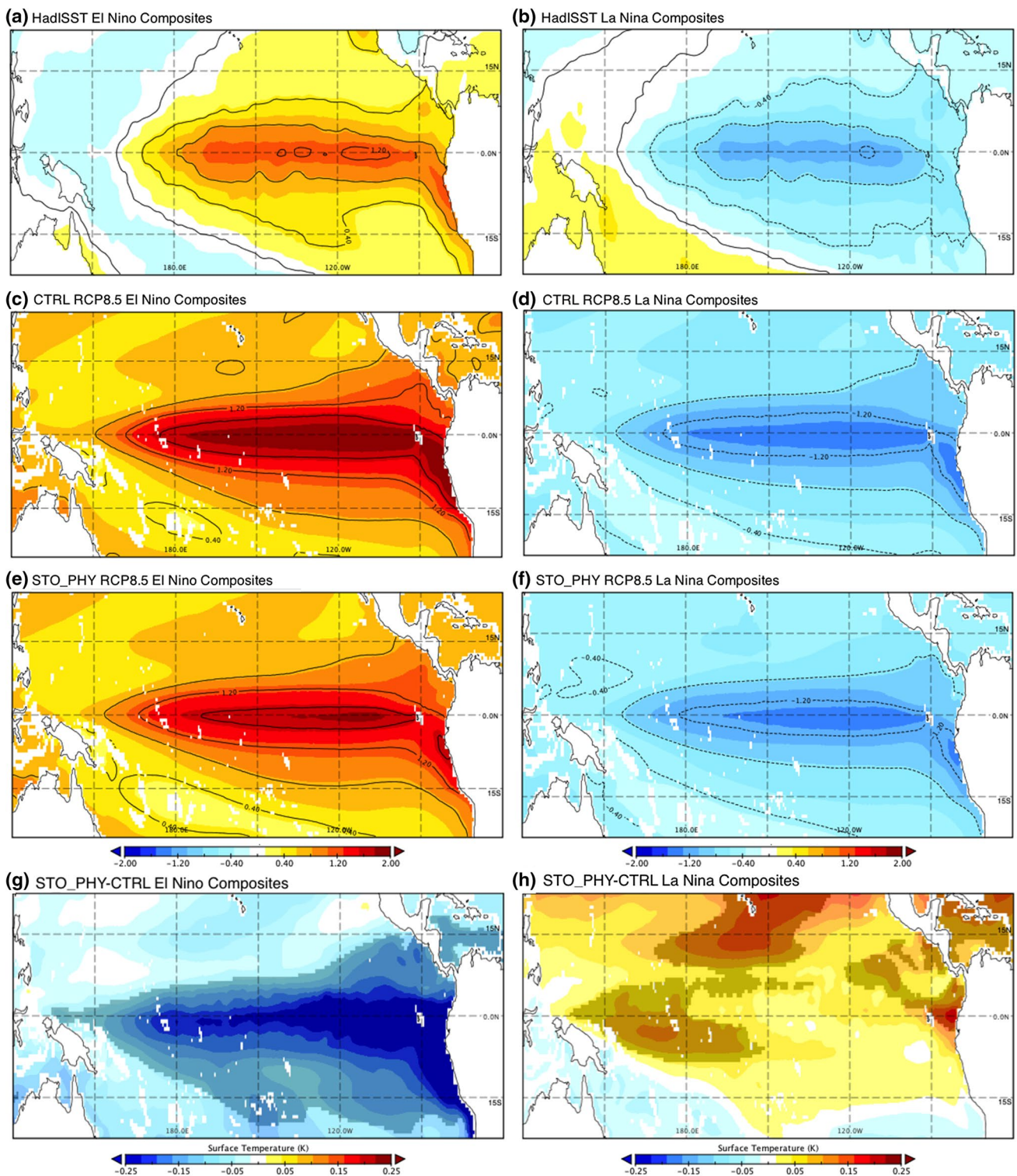


**Fig. 9** Sea surface temperature (SST) composites of El Niño events in **a** HadISST1, **c** CTRL RCP 8.5 and **e** STO\_PHY RCP 8.5 runs and composites of La Niña events in **b** HadISST1, **d** CTRL RCP 8.5 and **f** STO\_PHY RCP 8.5 runs. Difference between CTRL and HadISST for El Niño (**g**) and La Niña (**h**) composites. Difference between

STO\_PHY and CTRL for El Niño indicated both in contours and shades and La Niña composites Grey shaded in **g** and **h** show where differences are significantly different from zero above the 95% level according to the Student t-test

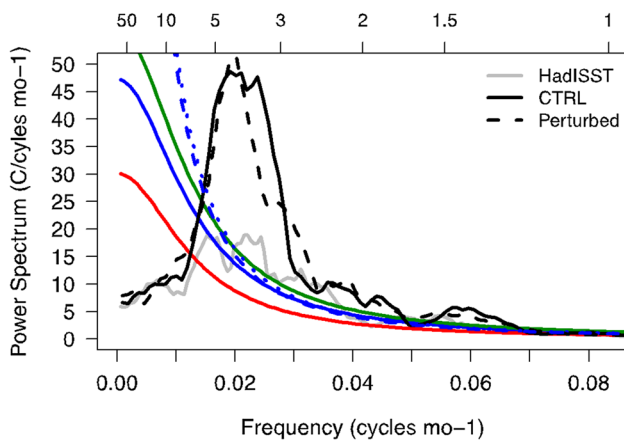


**Fig. 10** As Fig. 4 but for CTRL\_RCP8.5 (black solid), STO\_PHY\_RCP8.5 (black dashed) and HadISST1 (grey solid). The best fit AR(1) spectrum (red) and its 95% (blue) and 99% (green) confidence bounds for HadISST. Dashed and dotted blue lines are 95% confidence bounds for STO\_PHY and CTRL

stronger WWBs in the STO\_PHY simulations that have the potential to trigger more frequent and stronger El Niño events. The coupling between SST and winds strengthens with stochastic physics which, when combined with changes of WWBs, it is likely responsible for the improvement of ENSO representation in EC-Earth climate coupled model. Previous studies showed that with stochastic physics the representation of Madden-Julian Oscillation (MJO) is improved in terms of amplitude and frequency, and the improvement of MJO may also favour the improvement of ENSO due to the interaction of ENSO and MJO (Kessler and Kleeman 2000; Vitart and Molteni 2010; Vitart et al. 2003). In this study we propose that the increase of WWB with implementation of stochastic physics triggers more ENSO events. However, we need to bear in mind that the interaction between MJO and ENSO could also contribute to the improvement of ENSO with stochastic physics.

The implementation of stochastic physics not only improves the representation of ENSO in EC-Earth but also the model mean state. This has been highlighted by Berner et al. (2017) as a potential benefit of stochastic parameterization schemes. EC-Earth has a warm SST bias in the western and northern tropical Pacific, as well as off the west coast of South America, but cold biases in the central tropical Pacific Ocean across a wide range of longitudes. With stochastic physics, the warm biases in the western tropical Pacific Ocean are reduced. Similar improvement is found also for precipitation. Previous studies already showed the interaction between the mean state and ENSO (Kim et al. 2014; Watanabe and Wittenberg 2012) suggesting that the SST biases in the tropical Pacific could be a possible reason for the weak ENSO in EC-Earth. One possibility is that the improvement of the mean ocean and atmospheric state

induced by the stochastic physics schemes is reducing the biases in coupled feedbacks in the tropical Pacific, consequently leading to an improvement in the ENSO representation. However, we should be aware that there might be other reasons for such improvement not connected with the mean state. In particular, the response of the zonal winds to SST perturbations has improved, as well as the distribution of westerly wind events. However, we also note that due the nonlinearity of the coupled feedback in the tropical Pacific, the improvement of ENSO could also lead to further improvements of the mean state.

The same set of analysis on the impact of the stochastic physics on ENSO is also applied to the future scenario experiments (RCP8.5 forcing), again looking at runs with and without stochastic physics. Compared to the historical experiments, the control RCP8.5 has larger warm SST anomalies as in the CCSM historical run that has large warm SST biases. The results show that in the EC-Earth RCP8.5 control experiments, the ENSO amplitude is much stronger and the power spectrum is sharp and narrow, i.e. is opposite to the ENSO behaviour in historical control experiments. With stochastic physics, the amplitude of ENSO is reduced. The prominent power spectrum around the period of 3–4.5 years is slightly reduced too. However, longer simulations or more ensemble members are needed to test its significance. The impact of the stochastic physics on the simulation of ENSO in EC-Earth future scenario experiments supports the argument that the mean state bias, associated with the coupled feedbacks bias in the tropics, could be responsible for the deficiency of the ENSO simulation in the climate coupled models.

Previous studies show that the biased representation of ENSO in climate coupled models is related to deficiencies in the simulation of the mean climate in the tropical Pacific (Lloyd et al. 2011; Watanabe and Wittenberg 2012). In this study both the representation of the mean state and that of ENSO are improved with the implementation of stochastic physics. However, the non-linear coupled system and the limited number and type of available experiments makes it difficult to determine which is the cause or the driver of the other (i.e. the improvement of ENSO causes the improvement of the mean state or vice versa) or both of them ameliorate in response to the implementation of stochastic physics.

The improvement of ENSO in both EC-Earth and CCSM (Christensen et al. 2017) gives us confidence that the improvement of ENSO with stochastic physics can be expected across models. It appears that the implementation of stochastic physics into the climate coupled model has the potential to improve simulations of the ENSO variability and amplitude whether the control model has an excessively strong or weak ENSO. The details of the mechanisms that explain how the stochastic physics affect ENSO are clearly dependent on the biases of the coupled climate models,



especially on the coupled feedback in the tropical Pacific. Nevertheless, it appears that the representation of unresolved sub-grid scale variability through stochastic physics schemes can interact with the resolved scales improving low frequency aspects of the simulated climate.

**Acknowledgements** Free data accessibility to the climate user community is granted through a dedicated THREDDS Web Server hosted by CINECA (<https://sphinx.hpc.cineca.it/thredds/sphinx.html>), where it is possible to browse and directly download all of the Climate SPHINX data used in the present work. Further details on the data accessibility and on the Climate SPHINX project itself are available on the official website of the project (<http://www.to.isac.cnr.it/sphinx/>). The authors acknowledge computing resources provided by LRZ and CINECA in the framework of Climate SPHINX and Climate SPHINX reloaded PRACE projects. Jost von Hardenberg acknowledges support from the European Union's Horizon 2020 research and innovation programme under Grant agreement 641816 (CRESCENDO). Hannah Christensen acknowledges support from the Natural Environment Research Council under Grant agreement NE/P018238/1. Susanna Corti and Chunxue Yang acknowledge support by the PRIMAVERA project, funded by the European Commission under Grant agreement 641727 of the Horizon 2020 research programme. We acknowledge the contribution of the C3S 34a Lot 2 Copernicus Climate Change Service project, funded by the European Union, to the development of software tools used in this work. The National Center for Atmospheric Research is sponsored by the National Science Foundation.

**Open Access** This article is distributed under the terms of the Creative Commons Attribution 4.0 International License (<http://creativecommons.org/licenses/by/4.0/>), which permits unrestricted use, distribution, and reproduction in any medium, provided you give appropriate credit to the original author(s) and the source, provide a link to the Creative Commons license, and indicate if changes were made.

## References

- Alder RF, Huffman GJ, Chang A, Ferraro R, Xie P-P, Janowiak J, Rudolf B, Schneider U, Curtis S, Bolvin D, Gruber A, Susskind J, Arkin P, Nelkin E (2003) The version-2 global precipitation climatology project (GPCP) monthly precipitation analysis (1979–Present). *J Hydrometeorol* 4:1147–1167
- An S, Ham Y, Kug J-S, Timmermann A, Choi J, Kang I-S (2010) The inverse effect of annual mean state and annual cycle changes on ENSO. *J Clim* 23:1095–1110
- Battisti DS, Hirst AC (1989) Interannual variability in the tropical atmosphere/ocean system: influence of the basic state, ocean geometry and nonlinearity. *J Atmos Sci* 6:1687–1712
- Berner J, Doblas-Reyes FJ, Palmer TN, Shutts G, Weisheimer A (2008) Impact of a quasi-stochastic cellular automaton backscatter scheme on the systematic error and seasonal prediction skill of a global climate model. *Philos Trans R Soc Lond* 366A:2561–2579. <https://doi.org/10.1098/rsta.2008.0033>
- Berner J, Jung T, Palmer TN (2012) Systematic model error: the impact of increased horizontal resolution versus improved stochastic and deterministic parameterizations. *J Clim* 25:4946–4962. <https://doi.org/10.1175/JCLI-D-11-00297.1>
- Berner J, Achatz U, Batte L, De La Camara A, Crommelin D, Christensen H, Colangeli M, Dolaptchiev S, Franzke CLE, Friederichs P, Imkeller P, Jarvinen H, Juricke S, Kitsios V, Lott F, Lucarini V, Mahajan S, Palmer TN, Penland C, Von Storch J-S, Sakradzija M, Weniger M, Weisheimer A, Williams PD, Yano J-I (2017) Stochastic parameterization: Towards a new view of weather and climate models. *Bull Am Meteorol Soc*. <https://doi.org/10.1175/BAMS-D-15-00268.1>
- Blanke B, Nedin JD, Gutzler D (1997) Estimating the effects of stochastic wind stress forcing on ENSO irregularity. *J Clim* 10:1473–1486
- Bouttier F, Vié B, Nuissier O, Raynaud L (2012) Impact of stochastic physics in a convection-permitting ensemble. *Mon Weather Rev* 140:3706–3721. <https://doi.org/10.1175/MWR-D-12-00031.1>
- Bove MC, Elsner JB, Landsea CW, Niu X, Brien JJO (1998) Effect of El Niño on U.S. landfalling hurricanes, revisited. *Bull Am Meteorol Soc* 79:2477–2482. [https://doi.org/10.1175/1520-0477\(1998\)079<2477:EOENOO.2.0.CO;2](https://doi.org/10.1175/1520-0477(1998)079<2477:EOENOO.2.0.CO;2)
- Buizza R, Miller M, Palmer TN (1999) Stochastic representation of model uncertainties in the ECMWF ensemble prediction system. *Q J R Meteorol Soc* 125:2887–2908. <https://doi.org/10.1002/qj.49712556006>
- Cane M, Zebiak SE (1985) The theory of El Niño and the Southern Oscillation. *Science* 228:1085–1087
- Cane MA, Minnich M, Zebiak SE (1990) A study of self-excited oscillations of the tropical ocean–atmosphere system. Part I: Linear analysis. *J Atmos Sci* 47:1562–1577
- Chang P, Ji L, Li H, Fliigel M (1996) Chaotic dynamics versus stochastic processes in El Niño–Southern Oscillation in coupled ocean–atmosphere models. *Physica D* 98:301–320
- Christensen HM, Berner J, Coleman D, Palmer TN (2017) Stochastic parameterization and the El Niño–Southern Oscillation. *J Clim* 30, 17–38. <https://doi.org/10.1175/JCLI-D-16-0122.1>
- Collins M, An S-I, Cai W, Ganachaud A, Guilyardi E, Jin F-F, Jochum M, Lengaigne M, Power S, Timmermann A, Vecchi G, Wittenberg A (2010) The impact of global warming on the tropical Pacific Ocean and El Niño. *Nat Geosci* 3:391–397. <https://doi.org/10.1038/ngeo868>
- Davini P, von Hardenberg J, Corti S, Christensen HM, Juricke S, Subramanian A, Watson PAG, Weisheimer A, Palmer TN, 2017, Climate SPHINX: evaluating the impact of resolution and stochastic physics parameterisations in climate simulations (**submitted**)
- Eisenman I, Yu LS, Tziperman E (2005) Westerly wind bursts: ENSO's tail rather than the dog? *J Clim* 18:5224–5238
- Fedorov AV (2002) The response of the coupled tropical ocean–atmosphere to westerly wind bursts. *Q J R Meteorol Soc* 128(579):1–23
- Fedorov AV, Hu S, Lengaigne M, Guilyardi E (2015) The impact of westerly wind bursts and ocean initial state on the development and diversity of El Niño events. *Clim Dyn* 44:1381–1401
- Flato G et al (2013) Evaluation of climate models. In: Stocker TF et al (eds) *Climate change 2013: the physical science basis*. Cambridge University Press, Cambridge, pp 741–866
- Flügel M, Chang P, Penland C (2004) The role of stochastic forcing in modulating ENSO predictability. *J Clim* 17: 3125–3140. [https://doi.org/10.1175/1520-0442\(2004\)017<3125:TROSEF.2.0.CO;2](https://doi.org/10.1175/1520-0442(2004)017<3125:TROSEF.2.0.CO;2)
- Gebbie G, Eisenman I, Wittenberg A, Tziperman E (2007) Modulation of westerly wind bursts by sea surface temperature: a semi-stochastic feedback of ENSO. *J Atmos Sci* 64:3281–3295
- Guilyardi E, Wittenberg A, Fedorov A, Collins M, Wang C, Capotondi A, van Oldenborgh GJ, Stockdale T (2009) Understanding El Niño in ocean–atmosphere general circulation models: progress and challenges. *Bull Am Meteorol Soc* 90:325–340. <https://doi.org/10.1175/2008BAMS2387.1>
- Ham Y-G, Kug J-S (2014) Effects of Pacific intertropical convection zone precipitation bias on ENSO phase transition. *Environ Res Lett* 9:064008 (8 pp)
- Jankov I, Berner J, Beck J, Jiang H, Olson JB, Grell G, Smirnova TG, Benjamin SG, Brown JM (2017) A performance comparison between multiphysics and stochastic approaches within a North American RAP ensemble. *Mon Weather Rev* 145:1161–1179. <https://doi.org/10.1175/MWR-D-16-0160.1>

- Jin F-F (1996) Tropical ocean–atmosphere interaction, the Pacific cold tongue, and the El Niño–southern oscillation. *Science* 274:76–78
- Jin F-F (1997a) An equatorial recharge paradigm for ENSO, I, Conceptual model. *J Atmos Sci* 54:811–829
- Jin F-F (1997b) An equatorial recharge paradigm for ENSO, II, A stripped-down coupled model. *J Atmos Sci* 54:830–845
- Kessler WS, Kleeman R (2000) Rectification of the Madden-Julian oscillation into the ENSO cycle. *J Clim* 13:3560–3575
- Kim ST, Cai W, Jin F-F, Yu J-Y (2014) ENSO variability in coupled climate models and its association with mean state. *Clim Dyn* 42:3313–3321
- Lengaigne M, Guilyardi E, Boulanger JP, Menkes C, Delecluse P, Inness P, Cole J, Slings J (2004) Triggering El Niño by westerly wind events in a coupled general circulation model. *Clim Dyn* 23:601–620
- Levine AFZ, Jin F-F, McPhaden MJ (2016) Extreme noise–extreme El Niño: how state-dependent noise forcing creates El Niño–La Niña asymmetry. *J Clim* 29:5483–5499. <https://doi.org/10.1175/JCLI-D-16-0091.1>
- Lin JW-B, Neelin JD (2000) Influence of a stochastic moist convective parametrization on tropical climate variability. *Geophys Res Lett*, 27, 3691–3694. <https://doi.org/10.1029/2000GL011964>
- Lin J, Neelin JD (2003) Towards stochastic deep convective parametrization in general circulation models. *Geophys Res Lett* 30:1162. <https://doi.org/10.1029/2002GL016203>
- Lloyd J, Guilyardi E, Weller J (2011) The role of atmosphere feedbacks during ENSO in the CMIP3 models, Part II: using AMIP runs to understand the heat flux feedback mechanisms. *Clim Dyn* 37:1271–1292
- Luo J-J, Masson S, Behera S, Shingu S, Yamagata T (2005) Seasonal climate predictability in a coupled OAGCM using a different approach for ensemble forecasts. *J Clim* 18:4474–4497
- Madec G (2008) NEMO ocean engine, 2008. In: Technical report, Institute Pierre-Simon Laplace (IPSL)
- Münich M, Cane MA, Zebiak SE (1991) A study of self-excited oscillations of the tropical ocean–atmosphere system. Part II: Nonlinear case. *J Atmos Sci* 48: 1238–1248. [https://doi.org/10.1175/1520-0469\(1991\)048<1238:ASOSEO.2.0.CO;2](https://doi.org/10.1175/1520-0469(1991)048<1238:ASOSEO.2.0.CO;2)
- Neale RB, Richter JH, Jochum M (2008) The impact of convection on ENSO: from a delayed oscillator to a series of events. *J Clim* 21: 5904–5924. <https://doi.org/10.1175/2008JCLI2244.1>
- Neelin JD (1990) A hybrid coupled general circulation model for El Niño studies. *J Atmos Sci* 47:674–693
- Palmer TN, Buizza R, Doblas-Reyes F, Jung T, Leutbecher M, Shutts GJ, Steinheimer M, Weisheimer A (2009) Stochastic parametrization and model uncertainty. ECMWF tech rep 38. *J Clim* 30(598):1–44. <http://www.ecmwf.int/sites/default/files/elibrary/2009/11577-stochastic-parametrization-and-model-uncertainty.pdf>
- Penland C, Sardeshmukh PD (1995) The optimal growth of tropical sea surface temperature anomalies. *J Clim* 8:1999–2024
- Philander SGH (1990) *El Niño, La Niña, and the Southern Oscillation*. Academic Press, New York
- Philip SY, Collins M, van Oldenborgh GJ, van den Hurk BJJM (2010) The role of atmosphere and ocean physical processes in ENSO in a perturbed physics coupled climate model. *Ocean Sci* 6:441–459
- Rasmusson EM, Carpenter TH (1982) Variations in tropical sea surface temperature and surface wind fields associated with the Southern Oscillation/El Niño. *Mon Weather Rev* 110: 354–384. [https://doi.org/10.1175/1520-0493\(1982\)110<0354:VITSST.2.0.CO;2](https://doi.org/10.1175/1520-0493(1982)110<0354:VITSST.2.0.CO;2)
- Rayner NA, Parker DE, Horton EB, Folland CK, Alexander LV, Rowell DP, Kent EC, Kaplan A (2003) Global analyses of sea surface temperature, sea ice, and night marine air temperature since the late nineteenth century. *J Geophys Res* 108(D14):4407. <https://doi.org/10.1029/2002JD002670>
- Ropelewski CF, Halpert MS (1996) Quantifying Southern Oscillation—precipitation relationships. *J Clim* 9:1043–1059. [https://doi.org/10.1175/1520-0442\(1996\)009<1043:QSOPR.2.0.CO;2](https://doi.org/10.1175/1520-0442(1996)009<1043:QSOPR.2.0.CO;2)
- Sanchez C, Williams KD, Collins M (2016) Improved stochastic physics schemes for global weather and climate models. *Q J R Meteorol Soc* 142:147–159. <https://doi.org/10.1002/qj.2640>
- Sarachik ES, Cane MA (2010) *The El Niño–Southern Oscillation phenomenon*. Cambridge University Press, Cambridge
- Sardeshmukh PD, Penland C, Newman M (2001) Rossby waves in a stochastically fluctuating medium. In: Imkeller P, von Storch J-S (eds) *Stochastic climate models*. Birkhauser, Basel, pp 359–384
- Sardeshmukh PD, Penland C, Newman M (2003) Drifts induced by multiplicative red noise with application to climate. *Europhys Lett* 63:498–504. <https://doi.org/10.1209/epl/i2003-00550-y>
- Srifer RL, Timmermann A, Mann ME, Keller K, Goose H (2014) Improved representation of tropical Pacific Ocean—atmosphere dynamics in an intermediate complexity climate model. *J Clim* 27:168–185
- Stevenson SL (2012) Significant changes to ENSO strength and impacts in the twenty-first century: results from CMIP5. *Geophys Res Lett* 39:L17703. <https://doi.org/10.1029/2012GL052759>
- Stone L, Saparin PI, Huppert H, Price C (1998) El Niño chaos: the role of noise and stochastic resonance on the ENSO cycle. *Geophys Res Lett* 25: 175–178. <https://doi.org/10.1029/97GL53639>
- Suarez MJ, Schopf PS (1988) A delayed action oscillator for ENSO. *J Atmos Sci* 45:3283–3287. [https://doi.org/10.1175/1520-0469\(1988\)045<3283:ADAOFE.2.0.CO;2](https://doi.org/10.1175/1520-0469(1988)045<3283:ADAOFE.2.0.CO;2)
- Sun Y, Sun DZ, Wu L et al (2013) Western Pacific warm pool and ENSO asymmetry in CMIP3 models. *Adv Atmos Sci* 30:940–953. <https://doi.org/10.1007/s00376-012-2161-1>
- Taylor K, Stouffer R, Meehl G (2012) An overview of CMIP5 and the experiment design. *Bull Am Meteorol Soc* 93:485
- Titchner HA, Rayner NA (2014) The Met Office Hadley Centre sea ice and sea surface temperature data set, version 2.1. Sea ice concentrations. *J Geophys Res Atmos* 119:2864–2889. <https://doi.org/10.1002/2013JD020316>
- Timmermann A, An S-I, Kug J-S, Jin F-F, Cai W, Capotondi A, Cobb K, Lengaigne M, McPhaden MJ, Stuecker MF, Stein K, Wittenberg AT, Yun K-S, Bayr T, Chen H-C, Chikamoto Y, Dewitte B, Dommenger D, Grothe P, Guilyard E, Ham Y-G, Hayashi M, Ineson S, Kang D, Kim S, Kim W, Santoso A, Takahashi K, Todd A, Wang G, Wang G, Xie R, Yang W-H, Yeh S-W, Hoon J, Zeller E, Zhang X (2018) El Niño–Southern Oscillation complexity. *Nature* 559:535–545
- Valcke S (2013) The OASIS3 coupler: a European climate modelling community software. *Geosci Model Dev* 6:373
- Vancoppenolle M, Bouillon S, Fichet T, Goosse H, Lecomte O, Morales Maqueda M, Madec G (2012) LIM, the Louvain-la-Neuve sea ice model, notes du pôle de modélisation
- Vecchi G, Harrison DE (2000) Tropical Pacific sea surface temperature anomalies, El Niño, and equatorial westerly wind events. *J Clim* 13:1814–1830
- Vitart F, Molteni F (2010) Simulation of the Madden–Julian oscillation and its teleconnections in the ECMWF forecast system. *Q J R Meteorol Soc* 136:842–855
- Vitart FMA, Balmaseda L, Ferranti, Anderson D (2003) Westerly wind events and the 1997/98 El Niño event in the ECMWF seasonal forecasting system: a case study. *J Clim* 16:3153–3170
- Watanabe M, Wittenberg AT (2012) A method for disentangling El Niño–mean state interaction. *Geophys Res Lett* 39:L14702
- Watanabe M, Kug J-S, Jin F-F, Collins M, Ohba M, Wittenberg A (2012) Uncertainty in the ENSO amplitude change from the past to the future. *Geophys Res Lett* 39:L20703
- Weisheimer A, Corti S, Palmer TN, Vitart F (2014) Addressing model error through atmospheric stochastic physical parametrizations: impact on the coupled ECMWF seasonal forecasting

- system. *Philos Trans R Soc Lond* 372A:20130290. <https://doi.org/10.1098/rsta.2013.0290>
- Wieners CE, de Ruijter WPM, Ridderinkhof W, von Der Heydt AS, Dijkstra HA (2016) Coherent tropical indo-pacific interannual climate variability. *J Clim* 29:4269–4291. <https://doi.org/10.1175/JCLI-D-15-0262.1>
- Williams PD (2012) Climatic impacts of stochastic fluctuations in air–sea fluxes. *Geophys Res Lett* 39:L10705. <https://doi.org/10.1029/2012GL051813>
- Wyrski K (1985) Water displacement in the Pacific and the genesis of El Niño cycles. *J Geophys Res* 90:7129–7132
- Xiang B, Wang B, Ding Q, Jin F-F, Fu X, Kim H-J (2012) Reduction of the thermocline feedback associated with mean SST bias in ENSO simulation. *Clim Dyn* 39(6):1413–1430. <https://doi.org/10.1007/s00382-011-1164-4>
- Yang C, Giese BS (2013) El Niño Southern Oscillation in an ensemble ocean reanalysis and coupled climate models. *J Geophys Res Oceans* 118:4052–4071. <https://doi.org/10.1002/jgrc.20284>
- Yeh S-W, Kirtman B (2006) Origin of decadal El Niño–Southern Oscillation-like variability in a coupled general circulation model. *J Geophys Res* 111:C01009. <https://doi.org/10.1029/2005JC002985>
- Yonehara H, Ujiie M (2011) A stochastic physics scheme for model uncertainties in the JMA one-week ensemble prediction system, CAS/JSC WGNE. *Res Activ Atmos Ocean Model* 41:69–10. <http://www.wcrp-climate.org/WGNE/BlueBook/2011/documents/author-list.html>
- Zebiak SE (1989) On the 30–60 day oscillation and the prediction of El Niño. *J Clim* 2:1381–1387
- Zhang T, Sun D-Z (2014) ENSO asymmetry in CMIP5. *J Clim* 27:4070–4093. <https://doi.org/10.1175/JCLI-D-13-00454.1>

**Publisher's Note** Springer Nature remains neutral with regard to jurisdictional claims in published maps and institutional affiliations.